Robustness of Complementary Wearable Ungrounded Antennas with respect to the Human-Body

Giovanni A. Casula[1], Giorgio Montisci[1], Andrea Michel[2], Paolo Nepa[2]

[1]*Dipartimento di Ingegneria Elettrica ed Elettronica, Università degli Studi di Cagliari, Piazza D'Armi, 09123 Cagliari, Italy*

[2] *Dipartimento di Ingegneria dell'Informazione, Università di Pisa, Pisa, Italy*

Corresponding author: Giovanni Andrea Casula (a.casula@diee.unica.it)

Robustness of Complementary Wearable Ungrounded Antennas with respect to the Human-Body

Several wearable antennas have been presented in the open scientific literature, showing a good robustness with respect to the body coupling effect, both on the input matching and on the antenna efficiency. In this work, we evaluate and compare the robustness with respect to the coupling with the human body of complementary structures. We focus on structures widely used as wearable antennas, namely the ungrounded meandered printed antennas (which are electric antennas), and the ungrounded meandered slot printed antennas (which are magnetic antennas). We will show that, although in non-wearable context these complementary structures are essentially equivalent, for wearable applications it is preferable to use magnetic antennas configurations, i.e. meandered slot printed antennas, because, by means of appropriate design choices, they can be far less sensitive to the proximity to the human body.

Keywords: Ungrounded antennas, Wearable antennas, Body-antenna coupling

1. INTRODUCTION

In the design of wearable antennas, the main difficulties are due to the strong coupling with the human body, which is a lossy and non-homogeneous material, and can significantly degrade the antenna performance (such as input impedance, resonant frequency, radiation efficiency) with respect to the case of free-space applications [1]. The wearable antenna performance is, in fact, very sensitive to the distance between the antenna and the body surface. In addition to this, in real-world applications this distance can randomly change during natural body movements [2]. Moreover, the electromagnetic and geometrical parameters of the antenna platform (the human body) not only change from person to person, but are different even for different locations of the antenna on the same person [3]. In wearable applications is therefore very important to limit the human body effect, and to resort to appropriate design choices able to improve the antenna robustness.

In [4], [5], and [6] a criterion has been proposed for the choice of the optimal shape and size of the antenna ground plane, able to enhance the robustness of UHF grounded wearable printed antennas with respect to the antenna-body coupling effects, relating the optimal ground plane shape to the position of the maxima of the electric and magnetic energy density distributions in the near field region around the antenna. Through a deep analysis of these distributions, we demonstrated that the degradation of the antenna performance, due to the proximity of the human body, can be reduced if the ground plane is modified aiming to confine the electric energy density in the region far from the antenna border.

These concepts have been extended also for the case of ungrounded antennas [7], where the absence of a metallic ground plane makes the structure even more sensitive to the

human body proximity effect. In [7], in order to improve the robustness of "ungrounded" printed wearable antennas with respect to the distance from the human body, an energy-based design criterion has been provided, which consists in a suitable choice of the antenna layout able to confine the electric energy density far from the antenna borders.

In this work, the energy-based design criterion for "ungrounded" printed wearable antennas described in [7], which relates the robustness of the structure with the position of the maxima of the electric and magnetic energy density distributions in the near field region around the antenna, is exploited to study the robustness with respect to the coupling with the human body of complementary structures. As a matter of fact, in free-space applications complementary antennas are considered almost equivalent [8]. This is not true for on-body applications, as the two complementary antennas are actually one "magnetic" and the other one "electric". Therefore, we expect a completely different robustness.

We focus here on two complementary antennas, quite popular for wearable applications:

a) the ungrounded printed meander line antennas (which are electric antennas) [9-14]

b) the ungrounded meandered slot printed antennas (which are magnetic antennas) [15-20].

Meander line antennas (MLAs) are an attractive, and very common, choice in the UHF band, since they allow to reduce antenna size, especially for RFID applications [11, 12]. Moreover, the meandered configuration allows the dipole to assume a suitable inductive input reactance, necessary to match the tag antenna with the chip storing the information. If the dipole arms are folded in meanders [10], the equivalent wire configuration shows both capacitive and inductive reactance, which mutually cancel. This behavior produces resonances at frequencies which can be significantly lower than in the case of straight wire antenna of the same height (and this frequency can be controlled by the number and depth of the meanders). On the other hand, the meandered antenna shows a narrower bandwidth and a lower gain, also due to the fact that usually the meandered antenna must be contained within a very small size (for example, a few centimeter-side square for a RFID tag which labels small objects).

In many applications, the MLAs are replaced by their complementary antenna, the Meandered Slot Antenna (MSA) [15-20]. The antenna layout of a typical MSA consists of a planar patch (without ground plane), on which a non-uniform slot-line is cut, occupying only a small part of the metallization. In this antenna, the main radiating element is the slot-line, and therefore it can be defined as a "magnetic antenna", and is complementary to the MLA, which is, on the other hand, an "electric antenna", wherein the radiating element is the metallic meandered dipole.

For RFID applications [15], the choice of MSAs, and, hence, of the slot as main radiating element, allows simplifying the synthesis of the inductive reactance, which is typically required to match the tag antenna with the capacitive impedance of the tag microchip. In each short slot-line portion of the MSA, which contributes with its irradiation to the radiated field, there is an electric energy accumulation, whereas the discontinuity (tooth) between two MSA having different cross-section (as shown in Figure 1), besides contributing to the radiated field, also adds an inductive reactance to the antenna input reactance [15]. Therefore, the whole slot profile of the MSA can be considered as a slot-line impedance transformer, and its many degrees of freedom can

easily allow to match its input impedance to the complex conjugate of the Integrated Circuit (IC) impedance.

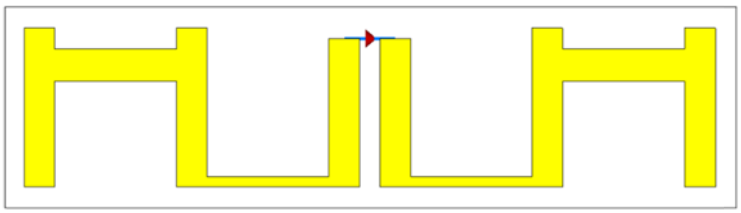

(a)

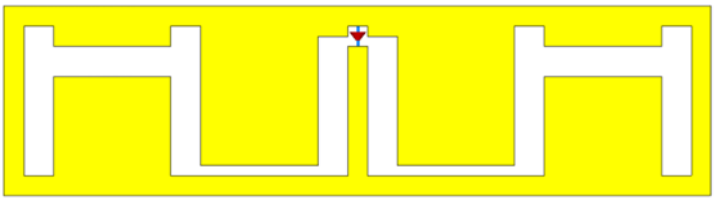

(b)

Figure 1. (a) Meander Line Antenna and its complementary (b) Meandered Slot Antenna

In the following section we compare the robustness of the complementary MLA and MSA antennas with respect to the coupling with the human body, showing that, for wearable applications, it is preferable to use magnetic antennas configurations, i.e. MSAs, because, by means of appropriate design choices, they can be less sensitive to the proximity to the human body. Moreover, typically the more robust antenna offers also a significantly better electromagnetic performance, as in the case that we report in this work.

2. NUMERICAL SIMULATION RESULTS

The relation between the performance of two complementary wearable ungrounded antennas (MLA and MSA) and their near-field energy distribution has been numerically investigated to analyze the antenna robustness with respect to the coupling with the human body.

In order to account for the presence of the human body, a simplified reference model of the human torso, defined as a stratified elliptical cylinder, and with physical parameters obtained from tissue database [7], has been considered in the simulated environment, and its dimensions are reported in Table I. The reported simulations are referred to the case of a thick man, which represents the worst case, since the larger absorption of a bigger torso will result in a lower value of the antenna efficiency.

TABLE I
PHYSICAL AND GEOMETRICAL PARAMETERS OF THE LAYERED ANATOMICAL MODEL AT 870 MHz

Layer	ε_r	σ [S/m]	Ellipse axis thin man [cm]	Ellipse axis thick man [cm]
Skin + fat	14.5	0.25	33.5 x 16.8	50.0 x 20.0
Muscle	55.1	0.93	31.0 x 14.2	46.5 x 17.0
Bone	20.8	0.33	28.4 x 10.5	42.6 x 12.6
Internal organs	52.1	0.91	27.2 x 8.4	41.0 x 10.0

We consider the following figures of merit to study the antenna robustness with respect to the body proximity, and to investigate the antenna performance when varying the antenna distance from the human body phantom, *d*:

- the radiation efficiency, η
- the power transmission coefficient, τ, expressed as:

$$\tau = 1 - \left| \frac{Z_{IN} - Z_0}{Z_{IN} + Z_0} \right|^2 \quad (1)$$

wherein Z_{IN} is the antenna input impedance, and Z_0 is a reference impedance.

In order to evaluate the robustness of different layouts by varying the body-antenna distance *d*, the reference impedance Z_0 has been chosen equal to the antenna input impedance at the frequency of 868 MHz, and when the antenna is adherent to the human body model (*d = 0 mm*).

The robustness of the proposed configurations has been studied separately for τ and $\tau \times \eta$, and the best configuration is considered to be the one exhibiting a reasonable value of $\tau \times \eta$, with a τ as great as possible, with both these parameters as stable as possible with respect to the antenna-body distance, *d*.

For both the considered antennas (MLA and MSA), three configurations have been investigated. In particular:

- **ANT** (the reference layout), which is the reference antenna
- **ANT-V**, in which the structure layout is extended toward the vertical direction;
- **ANT-H**, in which the structure layout is extended toward the horizontal direction.

2.1 MEANDERED SLOT ANTENNA

Following the layout described in [15], where a planar antenna layout suited to Sensor-RFID fabrication is presented, the MSA in Figure 1b has been designed to work in the

UHF frequency band at 868 MHz. The meander slot-line antenna lies on a high dielectric insulating layer, a silicon substrate ($\varepsilon r = 11.9$, and $\sigma = 0$) with a thickness of 4 mm, to electrically isolate the antenna from the skin, and the metallization thickness is equal to 0.035 mm.

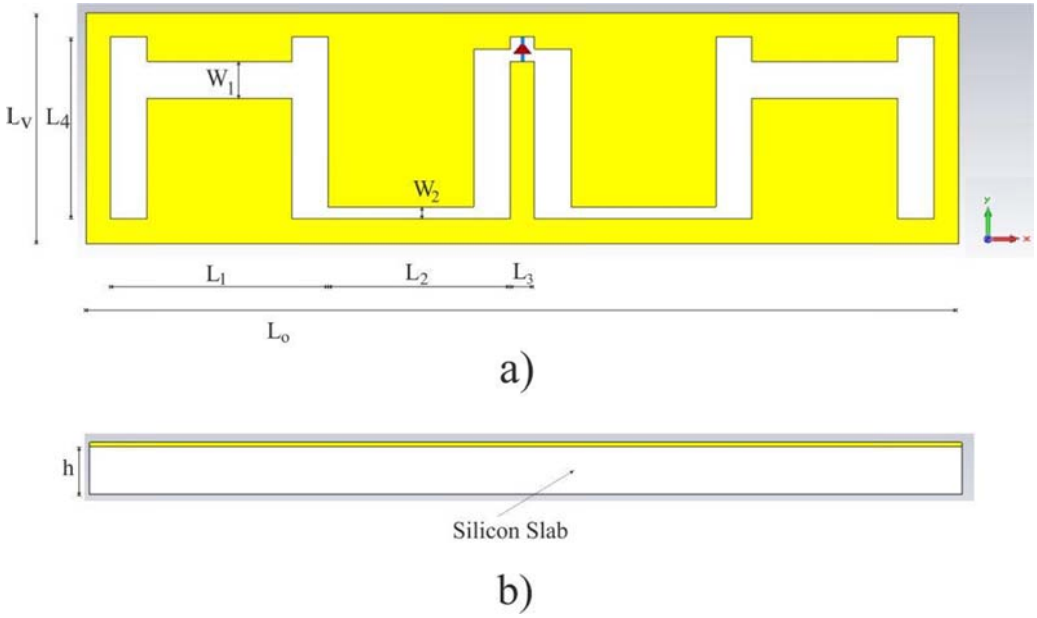

Figure 2. Layout of the analyzed meandered slot antenna. (a) Top view; (b) Side view. Lo = 72 mm, LV = 19 mm, L1 = 18 mm, L2 = 15 mm, L3 = 2 mm, L4 = 15 mm, W1 = 3 mm, W2 = 1 mm, h = 4 mm.

The geometry of the MSA, and its geometrical parameters, are reported in Figure 2. In Figure 3, the distribution of the electric and magnetic energy densities is shown, evaluated in the antenna substrate. The electric energy density shows peaks towards the vertical direction, whereas the peaks of the magnetic energy density are directed towards the horizontal direction, each one close to the antenna lateral edges. Therefore, in this case, the analyzed configuration is characterized by a clear separation between the maxima of the electric energy density and the maxima of the magnetic energy density, and this physical distribution of the electromagnetic energy allows to significantly increase the antenna robustness with respect to the human body coupling by enlarging the structure (metallic patch and dielectric substrate) towards the direction of the maxima of the electric energy density.

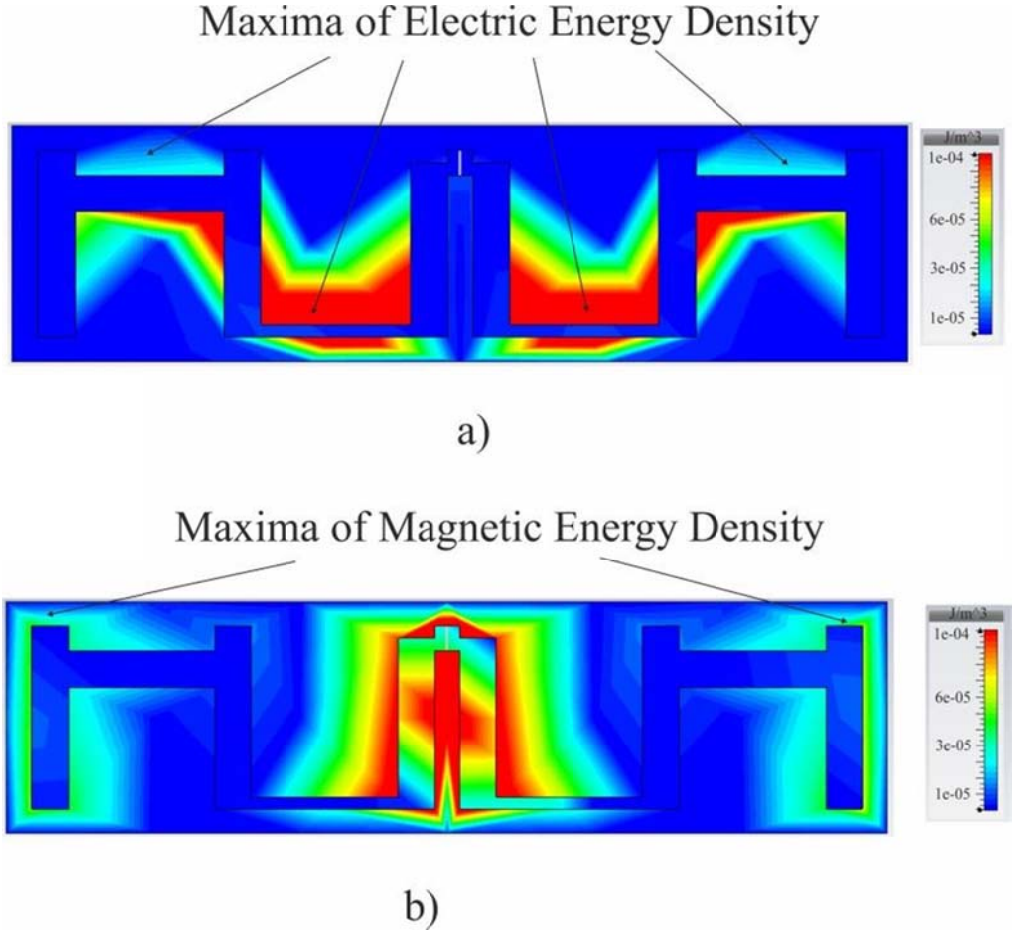

Figure 3. Electric (a) and magnetic (b) energy density for the antenna shown in Figure 2, in free space. Energy densities are evaluated in the antenna dielectric substrate.

In order to show this behavior, two modified layouts have been obtained by adding an extension of the metallic patch and of the silicon substrate toward the direction where the peaks of the electric and magnetic energy density appear, respectively. Starting from the reference layout shown in Figure 2 (namely **ANT** configuration), the **ANT-V** configuration, shown in Figure 4a, is obtained with an extension of the structure equal to ΔL_V towards the vertical direction, whereas the **ANT-H** configuration, shown in Figure 4b, is obtained with an extension of the structure equal to ΔL_H towards the horizontal direction.

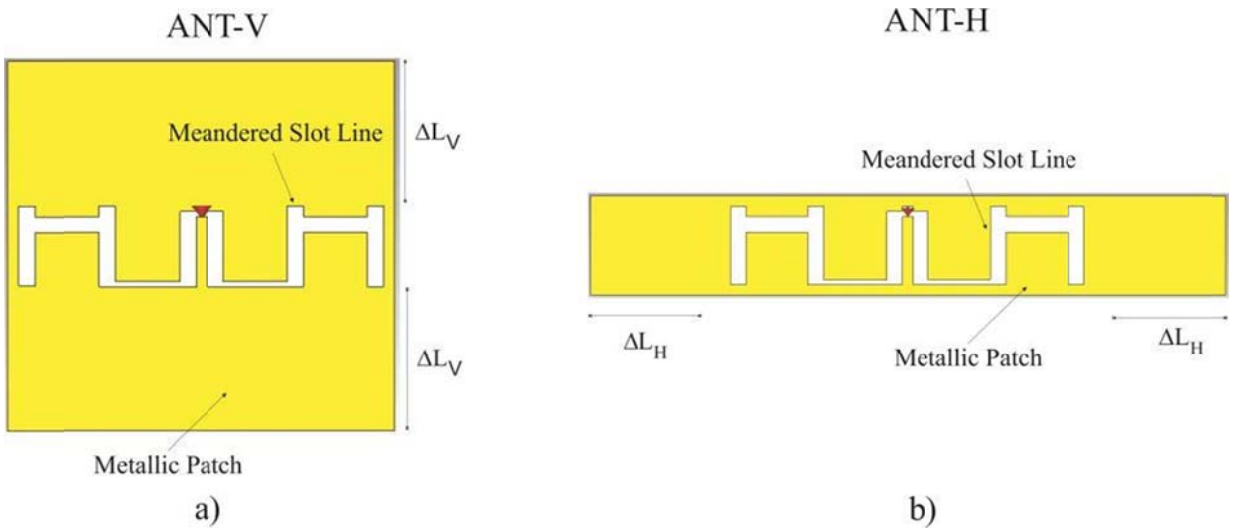

Figure 4. Meandered Slot Antenna in [15] with the substrate and the metallization extended toward the vertical direction (ANT-V) (a); Meandered slot antenna in [15] with the substrate and the metallization extended toward the horizontal direction (ANT-H) (b).

The size of ΔL_V and ΔL_H, which should be as small as possible in order to obtain a wearable antenna that is unobtrusive, compact, and comfortable to the user, has been chosen equal to 25 mm. However, we tested also the antenna configurations for variations of ΔL_V and ΔL_H from 10 to 35 mm, experimenting a similar behavior, but with the robustness of the antenna **ANT-V** which increases for increasing values of the enlargement ΔL_V.

The variation against d of τ, η, and $\tau \times \eta$ is shown in Figure 5a, 5b, and 5c, respectively. The **ANT-V** configuration performs significantly better than the other two configurations, and its robustness with respect to the body-antenna distance variation is remarkable. As a matter of fact, considering the results shown in Figure 5, only the configuration **ANT-V** can be effectively used, since for the **ANT** and **ANT-H** configurations, τ rapidly decreases to values below 10% for a distance of a few mm from the human body, with a value of $\tau \times \eta$ below 1%. On the other hand, for the **ANT-V** configuration, the product $\tau \times \eta$ remains acceptable for distances from 0 to 50 mm from the human body, and with a mean value around 5%, which is a typical value for ungrounded antennas, considering the high absorption of the dispersive human tissues.

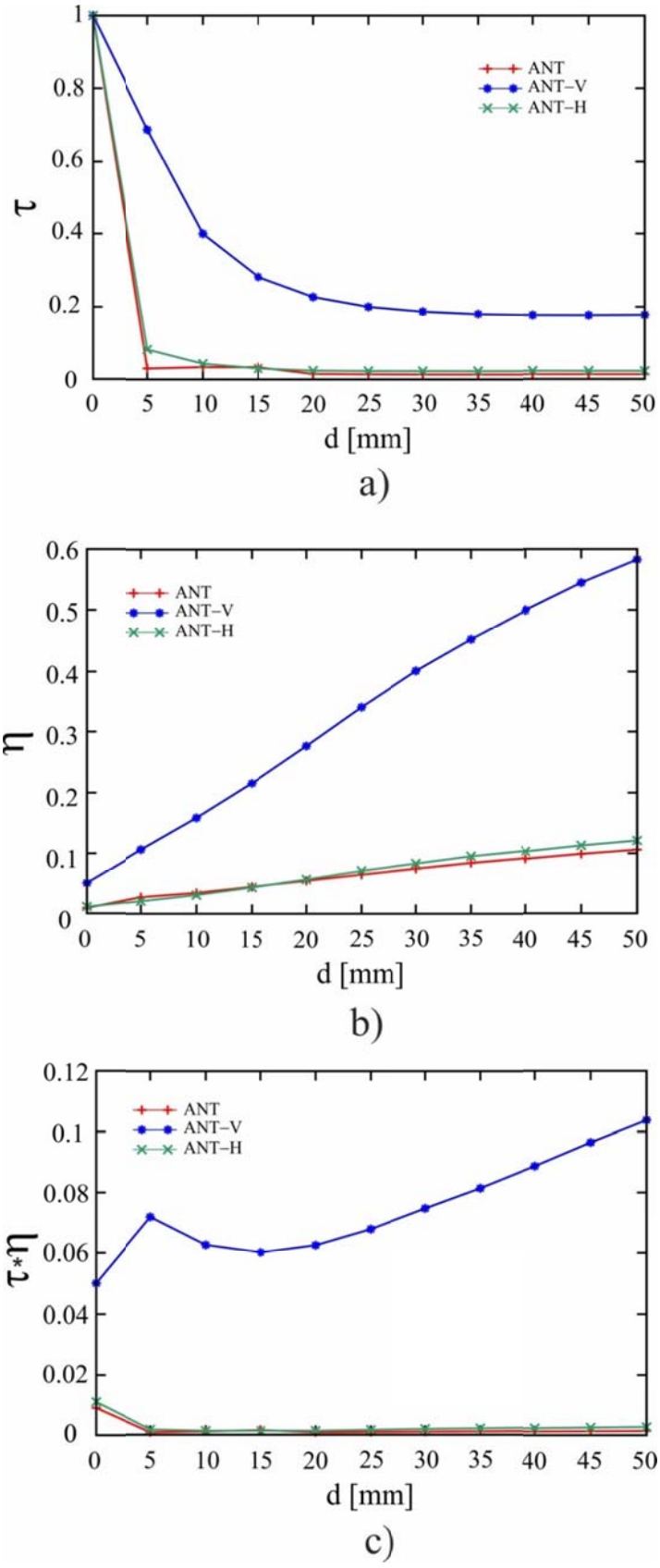

Figure 5. Variation of τ (a), η (b), and of the product τ × η (c), for the ANT, ANT-V, ANT-H antennas shown in Figure 2 and in Figure 4, at the design frequency of 868 MHz.

2.2 MEANDER LINE ANTENNA

In the UHF band, especially below 1 GHz, meander line antennas are very useful, since they allow to significantly reduce the antenna size. They are "electric antennas", because the radiation is due to the metallic arms of the folded dipole. In this section, we will analyze the robustness performances of a meander line antenna which is complementary to the "magnetic" MSA (Figure 2), described in the previous section. This single-layer, ungrounded wearable antenna, is attached onto the body through the same silicon substrate (with a dielectric constant equal to $\varepsilon r = 11.9$, and $\sigma = 0$), with a thickness of 4 mm. Figure 6 shows the layout of the analyzed meander line antenna.

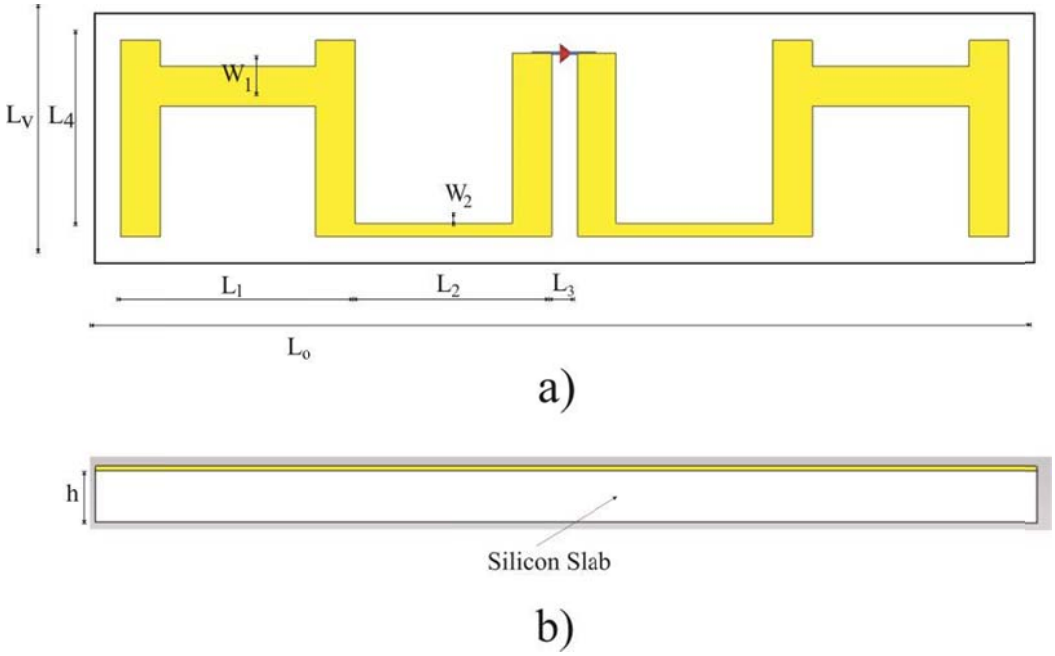

Figure 6. Layout of the meander line antenna. (a) Top view; (b) Side View. Lo = 69 mm, LV = 69 mm, L1 = 12.65 mm, L2 = 12.65 mm, L3 = 15 mm, L4 = 46 mm, L5 = 23 mm, h = 4 mm.

In Figure 7, the distribution of the electric and magnetic energy densities is shown, evaluated on the antenna substrate. For this antenna, the maxima of the electric energy density are not well separated from the maxima of the magnetic energy density, therefore we will show that incrementing the structure size has no effect on the antenna robustness, and that the coupling between the antenna and the human body remains almost the same. Also in this case, starting from the reference layout shown in Figure 6, and called **ANT** configuration (as explained in the previous sub-section), two modified layouts have been obtained, as indicated in Figure 8, by adding an extension of the silicon substrate toward the vertical direction (**ANT-V** configuration in Figure 8a, with a substrate extension ΔL_V), and toward the horizontal direction (**ANT-H** configuration in Figure 8b, with a substrate extension ΔL_H).

Again, we choose ΔL_V and ΔL_H equal to 25 mm, which corresponds to about half of the antenna original size, and for variations of ΔL_V and ΔL_H from 10 to 35 mm, we experimented a similar behavior of the analyzed antennas.

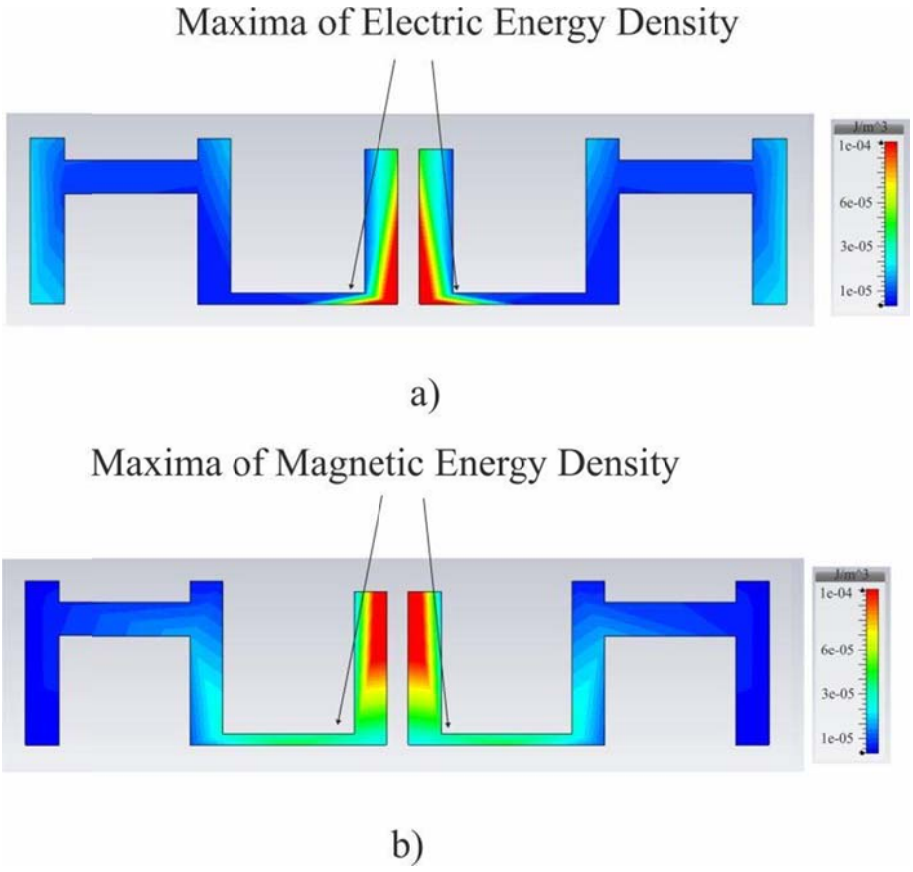

Figure 7. Electric (a) and magnetic (b) energy density for the antenna shown in Figure 6, in free space. Energy densities are evaluated in the antenna dielectric substrate.

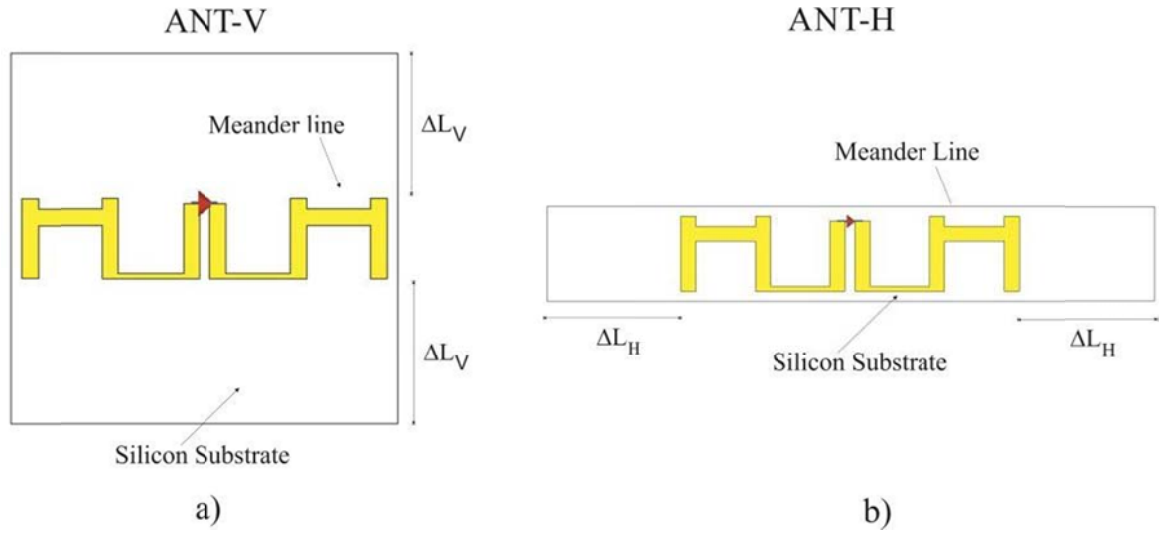

Figure 8. Meander line antenna with the substrate extended toward the vertical direction (ANT-V) (a); Meander line antenna with the substrate extended toward the horizontal direction (ANT-H) (b).

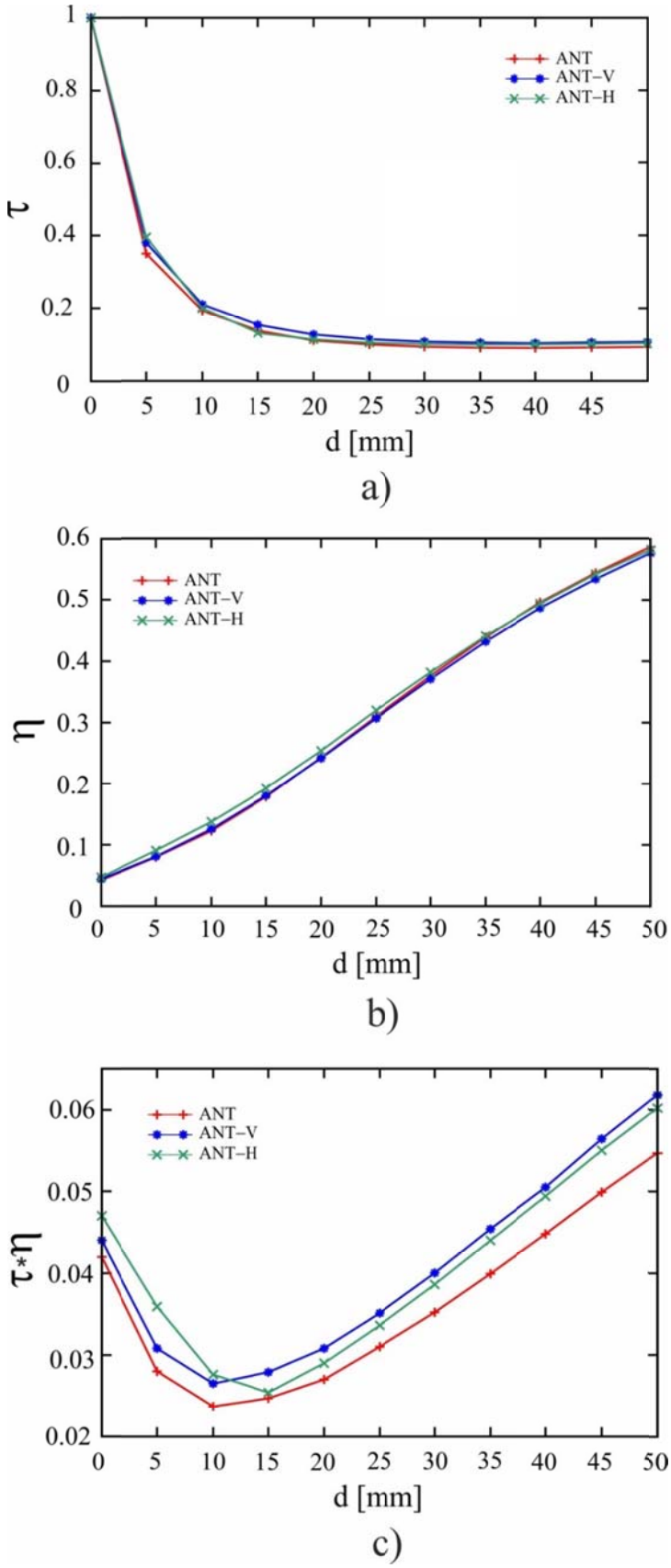

Figure 9. Variation of τ (a), η (b), and of the product τ × η (c), for the ANT, ANT-V, ANT-H antennas shown in Figure 6 and in Figure 8, at the design frequency of 868 MHz.

The variation against d of τ, η and $\tau \times \eta$ is shown in Figure 9a, 9b, and 9c, respectively. These results clearly indicate that the substrate enlargement has substantially no effect on the antenna robustness with respect to the human body coupling. As stated before, this is due to the fact that, for this antenna configuration, there is not a clear separation between the maxima of the electric energy density and the ones of the magnetic energy density. On the other hand, from the results presented in Figure 9, it is apparent that the antenna behavior experiences a significant degradation due to the coupling with the human body, with a power transmission coefficient, which decreases to less than 20% at a distance of only 10 mm from the human body phantom.

For wearable applications, the antenna size is a very strict requirement, and the wearable antenna should be as comfortable and unobtrusive as possible for the wearer. Therefore, it is very important to evaluate which should be the optimal extension, in terms of free space wavelength, required to design an antenna with an adequate robustness. In order to estimate the optimal enlargement of the structure, in Figure 10, a parametric analysis of the meander slot line antenna shown in Figure 2 has been performed, by varying the extension ΔL of the structure towards the vertical direction (which is the direction of the maxima of the electric energy density), as shown in Figure 4a for the ANT-V configuration. The simulations have been performed at the design frequency of 868 MHz. These results show that with an increment of the extension of only $\lambda/10$ for each side (λ being the free space wavelength at 868 MHz), the robustness of the antenna is significantly improved. On the other hand, when the size of the antenna is a critical issue, also smallest extensions can be used, still preserving an adequate robustness of the structure. As an example, also a minimal extension of $\lambda/20$ (corresponding to only 17.28 mm at 868 MHz), can ensure an usable antenna, at least if compared with the meander slot line antenna without any extension, which has a completely unsatisfying performance, both in terms of input matching and radiation efficiency (see Figure 5).

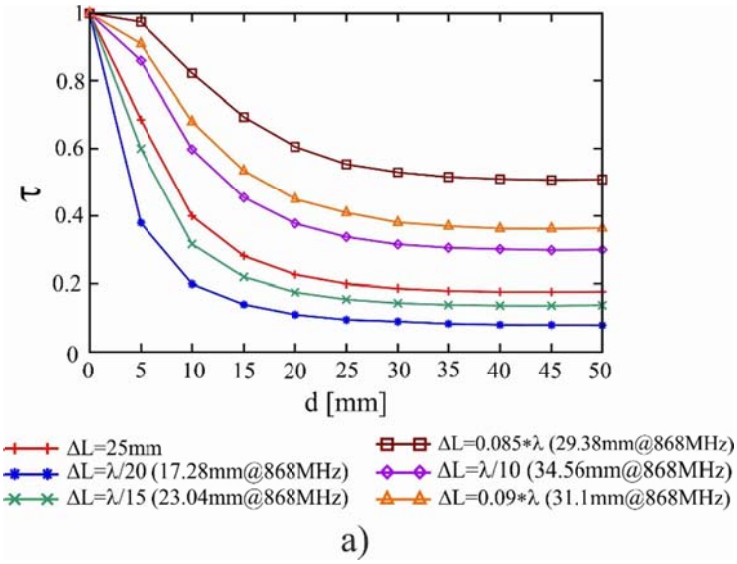

a)

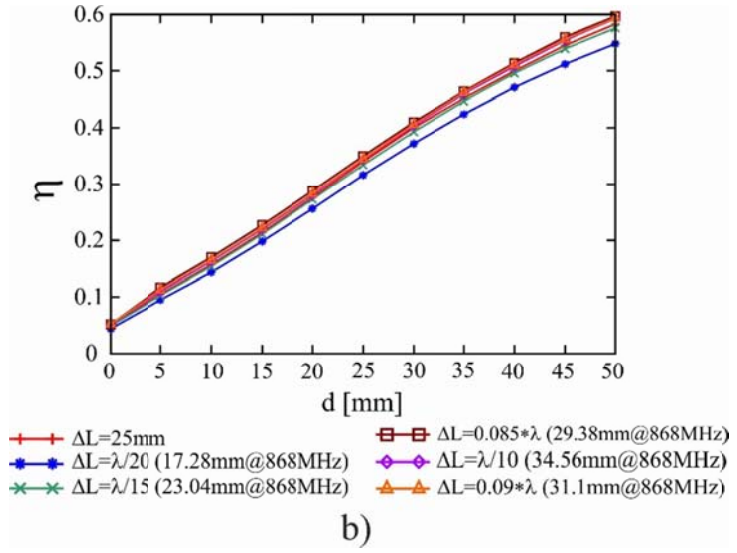

b)

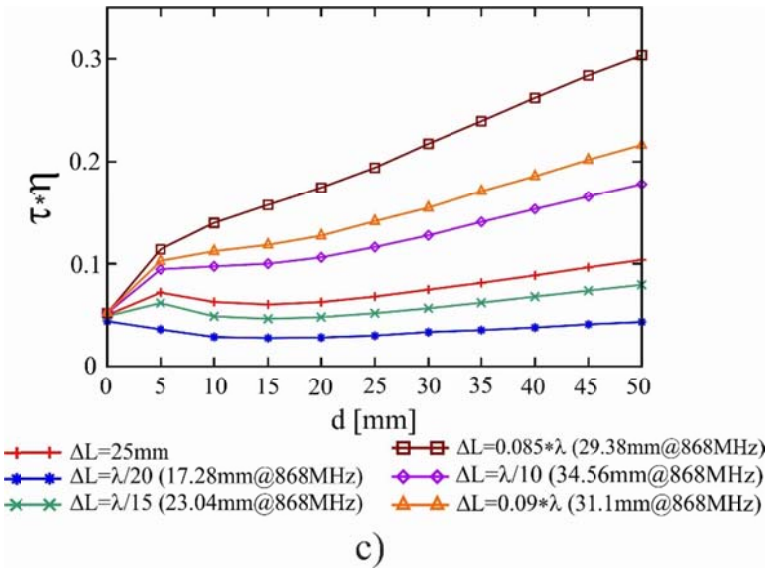

c)

Figure 10. Variation of τ (a), η (b), and of the product τ × η (c), for the ANT-V configuration of the Meandered Slot Line Antenna shown in Figure 4a, for different values of the extension of the structure *ΔL* towards the vertical direction. λ is the free space wavelength at the design frequency of 868 MHz.

The presented numerical analysis confirms that, since the human tissues are non-magnetic materials, the coupling between the "magnetic" MSA antenna and the human body can be reduced by enlarging the antenna structure towards the directions where the electrical energy density has a maximum. However, in this work we reached the very important conclusion that this approach, as proposed and described in [*7*], can be used only when the physical distribution of the electromagnetic energy in the antenna is such that there is a clear separation between the maxima of the electric energy density and the ones of the magnetic energy density. In particular, we have shown that in wearable applications "magnetic" antennas, like the MSA described in sub-section 2A, should be used, since they can be significantly more robust to the human body coupling with respect to their complementary "electric" antennas (like the MLA of sub-section 2B), whose sensitivity to the human body proximity cannot be easily improved.

3. CONCLUSION

This work describes a numerical investigation, based on the analysis of the electric and magnetic energy densities close to the borders of ungrounded antennas, to study the robustness with respect to the coupling with the human body of two complementary structures: the ungrounded meandered printed antenna (which is an electric antenna), and the ungrounded meandered slot printed antenna (which is a magnetic antenna). We have found that the design criterion used to improve the antenna robustness, leading to a proper enlargement of the antenna layout, is effective only if, in the antenna layout, the maxima of the electric energy density are well separated from the maxima of the magnetic energy density. As a consequence, the presented results show that it is possible to reduce the coupling with the human body only using the "magnetic" antenna, because, by means of appropriate design choices, they can be less sensitive to the proximity to the human body.

REFERENCES

[1] P.S. Hall, Y. Hao, V.I. Nechayev, A. Alomainy, C.C. Constantinou, C. Parini, M.R. Kamarudin, T.Z. Salim, D.T.M. Heel, R. Dubrovka, A.S. Owadall, W. Song, A.A. Serra, P. Nepa, M. Gallo and M. Bozzetti, "Antennas and Propagation for On-Body Communication Systems", IEEE Antennas and Propagation Magazine, vol. 49(3), pp. 41–58, 2007.

[2] A. Baroni, P. Nepa and H. Rogier, "A Reconfigurable Layout for a Self-Structuring Life-Jacket-Integrated Antenna of a SAR System" IEEE 2015 Antennas and Propagation Symposium, Vancouver, July 20-24, 2015.

[3] A. Michel, K. Karathanasis, P. Nepa and J.L. Volakis, "Accuracy of a Multi-probe Conformal Sensor in Estimating the Dielectric Constant in Deep Biological Tissues, to appear on IEEE Sensor Journal, 2015.

[4] G. A. Casula, A. Michel, P. Nepa, G. Montisci, and G. Mazzarella "Robustness of Wearable UHF-Band PIFAs to Human-Body Proximity", IEEE Trans. Antennas Propag., vol. 64, no. 5, May 2016.

[5] G. A. Casula, M. Altini, A. Michel and P. Nepa, "On the performance of low-profile antennas for wearable UHF-RFID tags," 1st URSI Atlantic Radio Science Conference, Gran Canaria, Spain, 2015

[6] M. Altini, G.A. Casula, G. Mazzarella, and P. Nepa, "Numerical investigation on the tolerance of wearable UHF-RFID tags to human body coupling", IEEE Antennas and Propagation Symposium, Vancouver, BC, Canada, July 20-24, 2015.

[7] G. A. Casula, A. Michel, G. Montisci, P. Nepa, and G. Valente, “Energy-Based Considerations for Ungrounded Wearable UHF Antenna Design”, IEEE Sensors Journal., vol. 17, no. 3, 2017.
[8] C. A. Balanis, “Antenna Theory: Analysis and Design”, John Wileys & Sons, Inc., 2005.
[9] G. Marrocco, "Gain-optimized self-resonant meander line antennas for RFID applications", IEEE Antennas Wireless Propag. Lett., vol. 2, pp. 302-305, 2003.
[10] T. J. Warnagiris and T. J. Minardo, “Performance of a meandered line as electrically small transmitting antenna,” IEEE Trans. Antennas Propagat., vol. 46, pp. 1797–1876, Dec. 1998.
[11] Rao, K.V.S., Nikitin, P.V., Lam, S.F., “Antenna design for UHF RFID tags: A review and a practical application”, IEEE Transactions on Antennas and Propagation, 53 (12), pp. 3870-3876, 2005.
[12] Travassos, X.L., Lisboa, A.C., Vieira, D.A.G., “Design of meander-line antennas for radio frequency identification based on multiobjective optimization”, International Journal of Antennas and Propagation, 2012, art. no. 795464.
[13] Braaten, B.D., Reich, M., Glower, J., “A compact meander-line UHF RFID tag antenna loaded with elements found in right/left-handed coplanar waveguide structures”, IEEE Antennas and Wireless Propagation Letters, 8, art. no. 5299014, pp. 1158-1161, 2009.
[14] Paredes, F., Zamora, G., Herraiz-Martínez, F.J., Martín, F., Bonache, J., “Dual-band UHF-RFID tags based on meander-line antennas loaded with spiral resonators”, IEEE Antennas and Wireless Propagation Letters, 10, art. no. 5960759, pp. 768-771, 2011.
[15] C. Calabrese, G. Marrocco, "Meandered-slot antennas for sensor-RFID tags", IEEE Antennas and Wireless Propagation Letters, vol. 7, pp. 5-8, 2008.
[16] Kim, J.-M., Kim, K.-W., Yook, J.-G., Park, H.-K., "Compact stripline-fed meander slot antenna", Electronics Letters, 37 (16), pp. 995-996, 2001.
[17] Allen, C.M., Eldek, A.A., Elsherbeni, A.Z., Smith, C.E., Huang, C.-W.P., Lee, K.-F., “Dual tapered meander slot antenna for radar applications”, IEEE Transactions on Antennas and Propagation, 53 (7), pp. 2324-2328, 2005.
[18] Kim, H., Yoon, Y.J., “Compact microstrip-fed meander slot antenna for harmonic suppression”, Electronics Letters, 39 (10), pp. 761-763, 2003.
[19] Gupta, A.K., Kumar, N., “Dual band meander slot antenna for mobile applications”, 2015 International Conference on Communication and Signal Processing (ICCSP 2015), Article number 7322609, Pages 828-830, India.
[20] Yang, C., Hua, G., Lu, P., Zhou, H., "Bow-tie shaped meander slot on-body antenna", International Symposium on Antennas and Propagation (ISAP) 2013, Volume 2, 2013, Article number 6717665, Pages 1013-1016, Nanjing (China).